

Fig. 38A-1-001. $\text{Te}(\text{OH})_6 \cdot 2\text{NH}_4\text{H}_2\text{PO}_4 \cdot (\text{NH}_4)_2\text{HPO}_4$ (TAAP). Projection of the crystal structure along the b direction [84Ave].

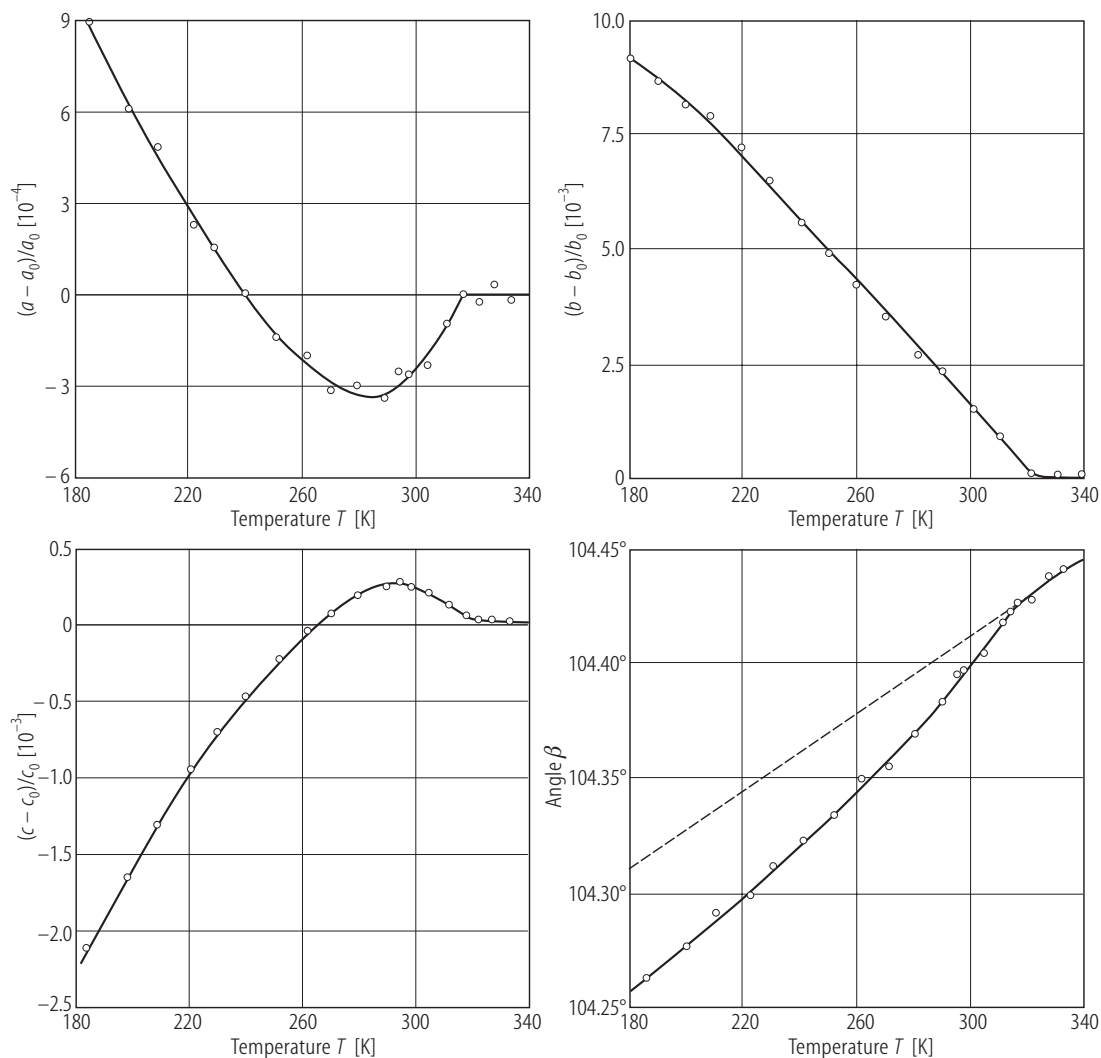


Fig. 38A-1-002. $\text{Te}(\text{OH})_6 \cdot 2\text{NH}_4\text{H}_2\text{PO}_4 \cdot (\text{NH}_4)_2\text{HPO}_4$ (TAAP). $(a - a_0)/a_0$, $(c - c_0)/c_0$, $(b - b_0)/b_0$, β vs. T [94Prz]. a_0 , b_0 , c_0 : extrapolated values of a , b , c , respectively, from the phase I.

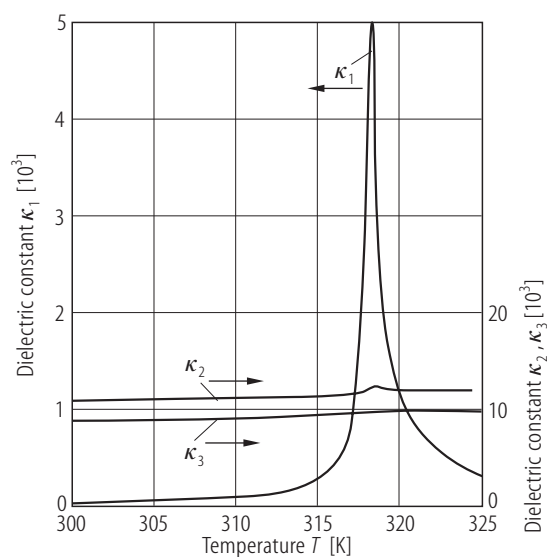


Fig. 38A-1-003. $\text{Te}(\text{OH})_6 \cdot 2\text{NH}_4\text{H}_2\text{PO}_4 \cdot (\text{NH}_4)_2\text{HPO}_4$ (TAAP). κ_1 , κ_2 , κ_3 vs. T [91Cza]. κ_1 : dielectric constant for E parallel to the polar direction, $\kappa_1 \approx \kappa_{(101)}$. $\kappa_2 = \kappa_b$. κ_3 : dielectric constant for E along the direction perpendicular to both the polar axis and the b axis.

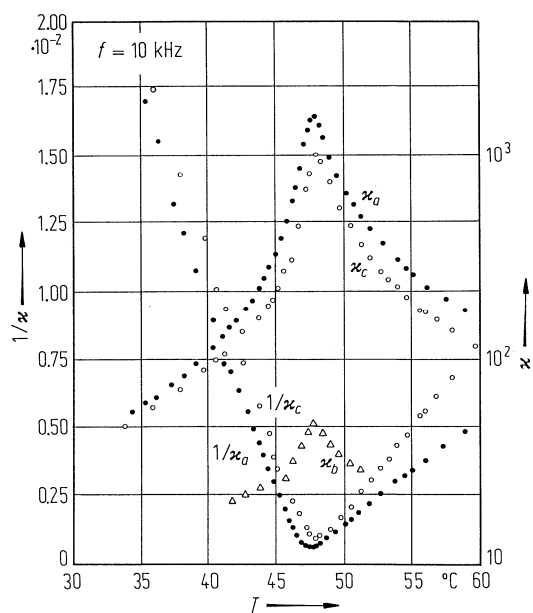


Fig. 38A-1-004. $\text{Te}(\text{OH})_6 \cdot 2\text{NH}_4\text{H}_2\text{PO}_4 \cdot (\text{NH}_4)_2\text{HPO}_4$ (TAAP). κ_a , κ_b , κ_c , κ_a^{-1} , κ_c^{-1} vs. T [84Gui].

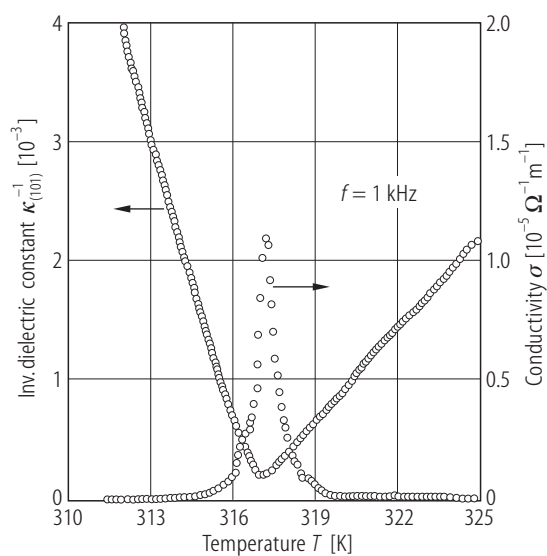


Fig. 38A-1-005. $\text{Te}(\text{OH})_6 \cdot 2\text{NH}_4\text{H}_2\text{PO}_4 \cdot (\text{NH}_4)_2\text{HPO}_4$ (TAAP). $\kappa_{(101)}^{-1}$, σ vs. T [90Cac]. $\kappa_{(101)}$: dielectric constant perpendicular to (101). σ : ac conductivity. $f = 1$ kHz.

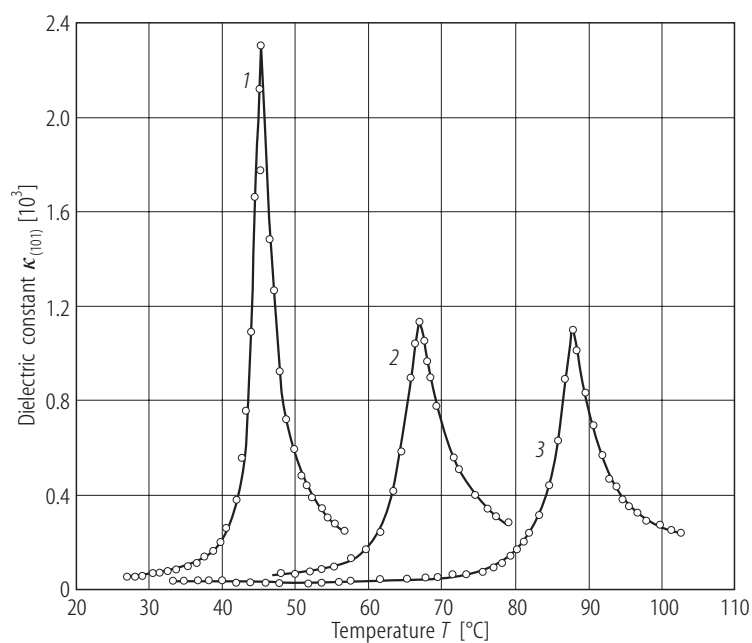


Fig. 38A-1-006. $[\text{Te}(\text{OH})_6 \cdot 2\text{NH}_4\text{H}_2\text{PO}_4 \cdot (\text{NH}_4)_2\text{HPO}_4]_1 - x[\text{Te}(\text{OD})_6 \cdot 2\text{ND}_4\text{D}_2\text{PO}_4 \cdot (\text{ND}_4)_2\text{DPO}_4]_x$. $\kappa_{(101)}$ vs. T [88Sha]. 1: $x = 0$, 2: partially deuterated, 3: $x \approx 1$. $\kappa_{(101)}$: dielectric constant for E perpendicular to (101) face.

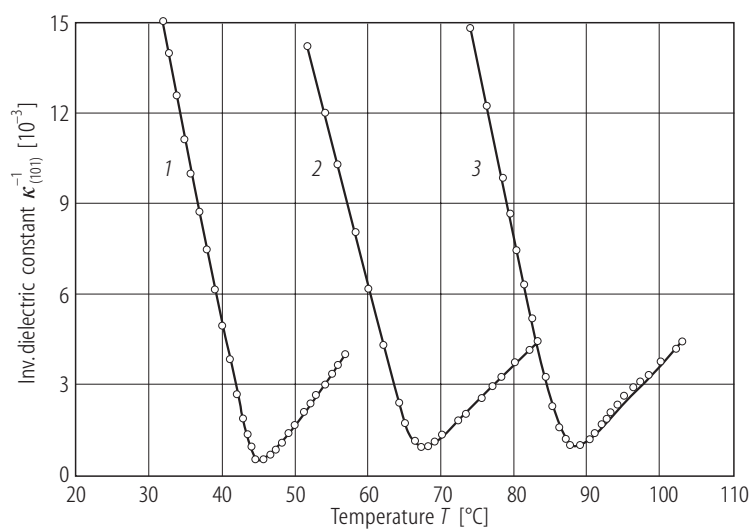


Fig. 38A-1-007. $[\text{Te}(\text{OH})_6 \cdot 2\text{NH}_4\text{H}_2\text{PO}_4 \cdot (\text{NH}_4)_2\text{HPO}_4]_1 - x[\text{Te}(\text{OD})_6 \cdot 2\text{ND}_4\text{D}_2\text{PO}_4 \cdot (\text{ND}_4)_2\text{DPO}_4]_x$. $\kappa_{(101)}^{-1}$ vs. T [88Sha]. 1: $x = 0$, 2: partially deuterated, 3: $x \approx 1$.

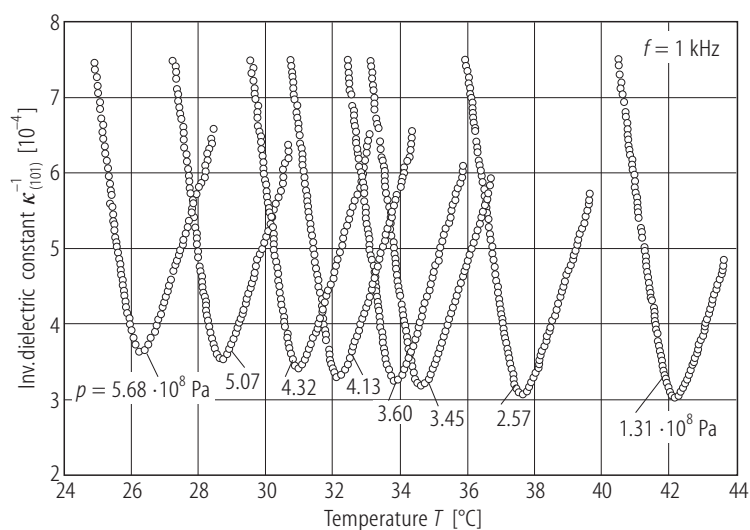


Fig. 38A-1-008. $\text{Te}(\text{OH})_6 \cdot 2\text{NH}_4\text{H}_2\text{PO}_4 \cdot (\text{NH}_4)_2\text{HPO}_4$ (TAAP). $\kappa_{(101)}^{-1}$ vs. T [96Fer]. Parameter: p .

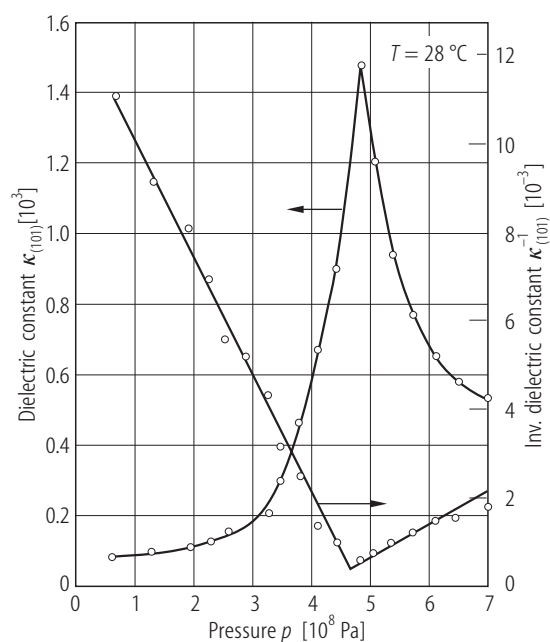


Fig. 38A-1-009. $\text{Te}(\text{OH})_6 \cdot 2\text{NH}_4\text{H}_2\text{PO}_4 \cdot (\text{NH}_4)_2\text{HPO}_4$ (TAAP). $\kappa_{(101)}$, $\kappa_{(101)}^{-1}$ vs. p [90Sha2]. $T = 28^\circ\text{C}$. $f = 10 \text{ kHz}$.

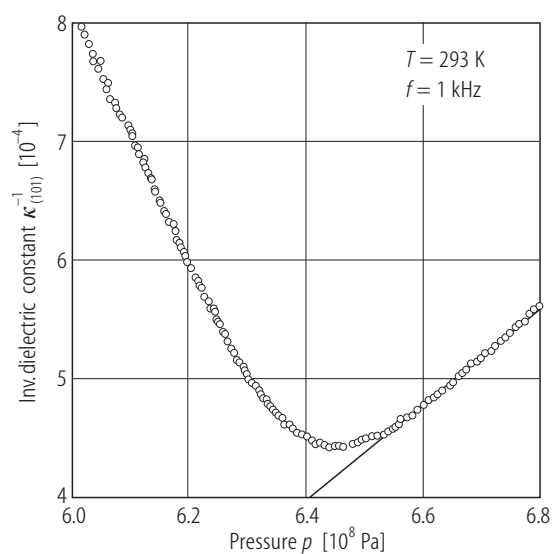


Fig. 38A-1-010. $\text{Te}(\text{OH})_6 \cdot 2\text{NH}_4\text{H}_2\text{PO}_4 \cdot (\text{NH}_4)_2\text{HPO}_4$ (TAAP). $\kappa_{(101)}^{-1}$ vs. p [96Fer]. $T = 293 \text{ K}$.

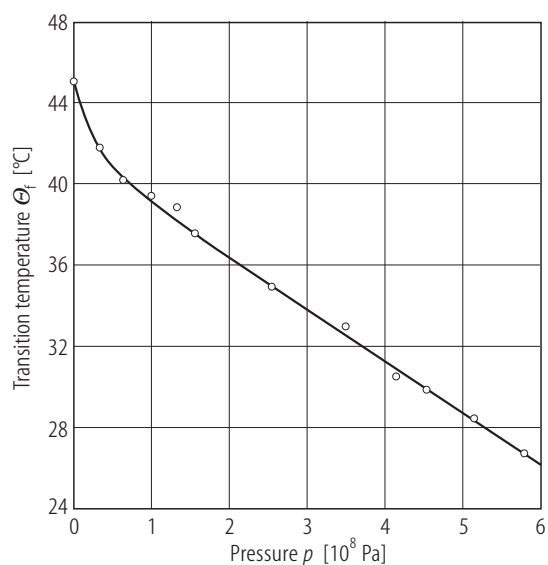


Fig. 38A-1-011. $\text{Te}(\text{OH})_6 \cdot 2\text{NH}_4\text{H}_2\text{PO}_4 \cdot (\text{NH}_4)_2\text{HPO}_4$ (TAAP). Θ_f vs. p [90Sha2].

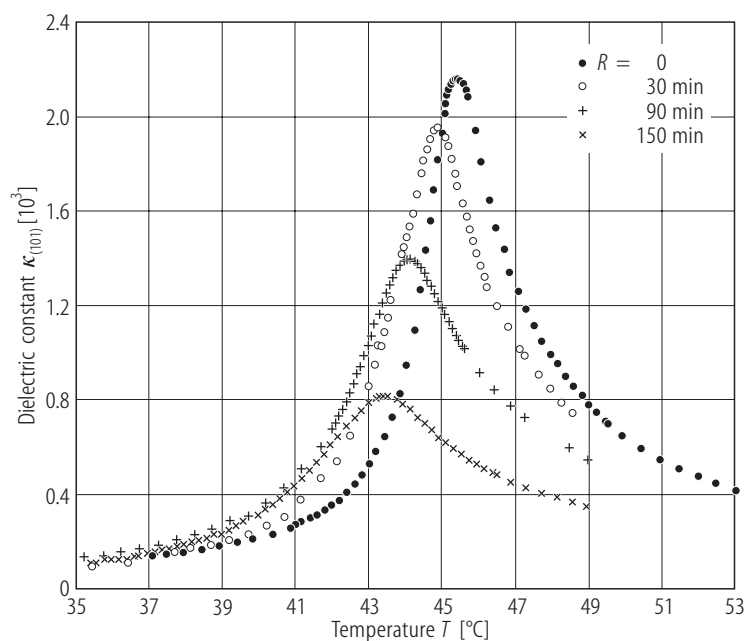


Fig. 38A-1-012. $\text{Te}(\text{OH})_6 \cdot 2\text{NH}_4\text{H}_2\text{PO}_4 \cdot (\text{NH}_4)_2\text{HPO}_4$ (TAAP). $\kappa_{(101)}$ vs. T [91Sha]. Parameter: R : irradiation time of X-ray. X-ray from Cu target of 38 kV, 25 mA was used.

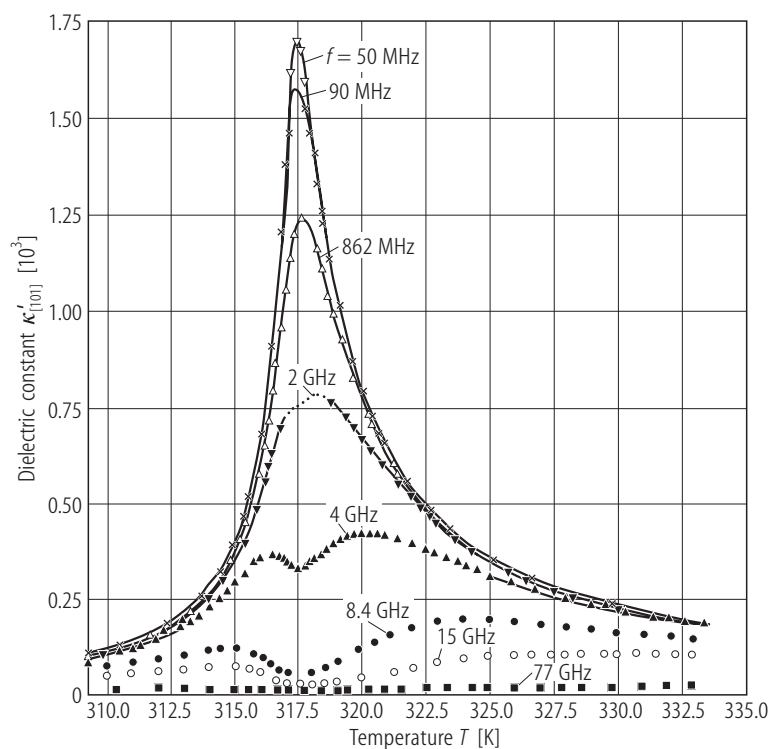


Fig. 38A-1-013. $\text{Te}(\text{OH})_6 \cdot 2\text{NH}_4\text{H}_2\text{PO}_4 \cdot (\text{NH}_4)_2\text{HPO}_4$ (TAAP). $\kappa'_{[101]}$ vs. T [92Sob]. Parameter: f . $\kappa'_{[101]}$: real part of dielectric constant for $\mathbf{E} \parallel [101]$.

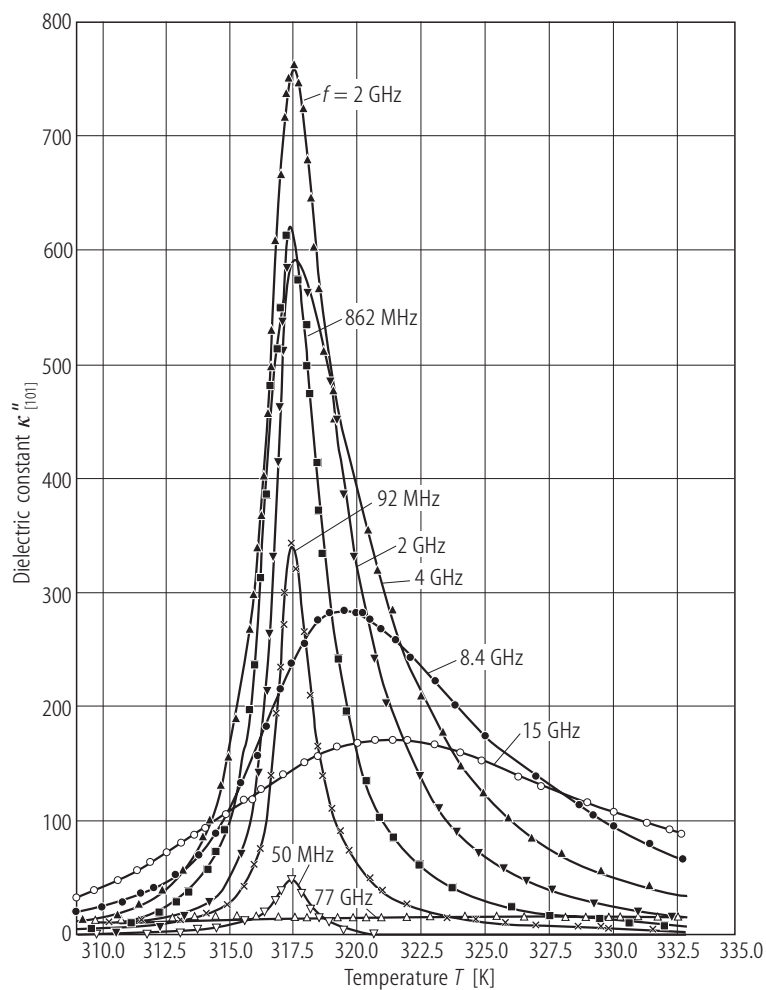


Fig. 38A-1-014. $\text{Te}(\text{OH})_6 \cdot 2\text{NH}_4\text{H}_2\text{PO}_4 \cdot (\text{NH}_4)_2\text{HPO}_4$ (TAAP). $\kappa''_{[101]}$ vs. T [92Sob]. Parameter: f . $\kappa''_{[101]}$: imaginary part of dielectric constant for $E \parallel [101]$.

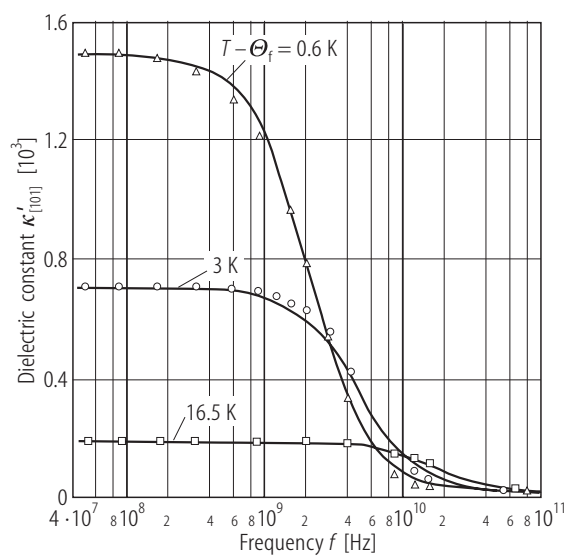


Fig. 38A-1-015. $\text{Te}(\text{OH})_6 \cdot 2\text{NH}_4\text{H}_2\text{PO}_4 \cdot (\text{NH}_4)_2\text{HPO}_4$ (TAAP). κ'_{101} vs. f [92Sob]. Parameter: $T - \Theta_f$.

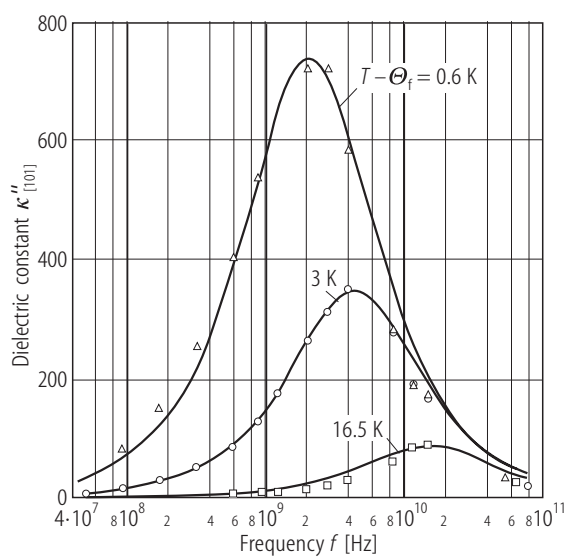


Fig. 38A-1-016. $\text{Te}(\text{OH})_6 \cdot 2\text{NH}_4\text{H}_2\text{PO}_4 \cdot (\text{NH}_4)_2\text{HPO}_4$ (TAAP). κ''_{101} vs. f [92Sob]. Parameter: $T - \Theta_f$.

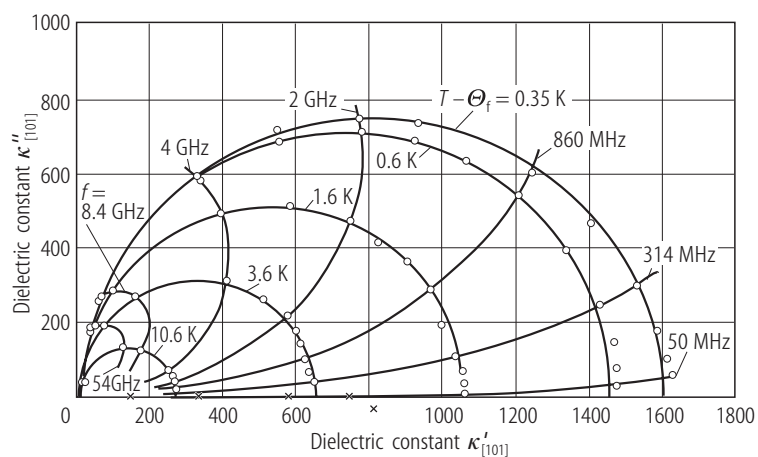


Fig. 38A-1-017. $\text{Te}(\text{OH})_6 \cdot 2\text{NH}_4\text{H}_2\text{PO}_4 \cdot (\text{NH}_4)_2\text{HPO}_4$ (TAAP). $\kappa'_{[101]}$ vs. $\kappa''_{[101]}$ (Cole-Cole diagram) [92Sob].
Parameter: $T - \Theta_f, f$. Cross: center of circular arc.

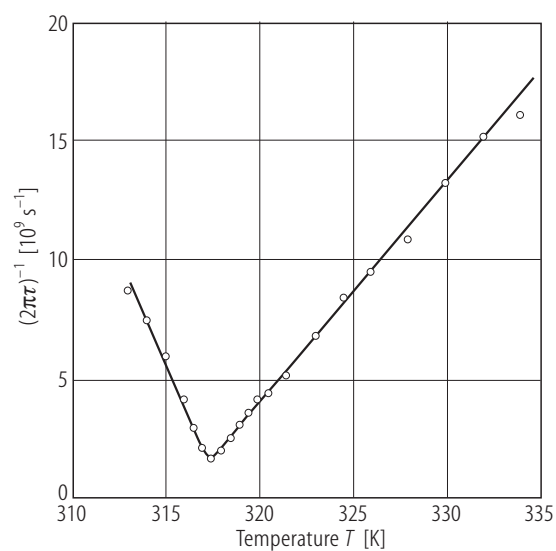


Fig. 38A-1-018. $\text{Te}(\text{OH})_6 \cdot 2\text{NH}_4\text{H}_2\text{PO}_4 \cdot (\text{NH}_4)_2\text{HPO}_4$ (TAAP). $(2\pi\tau)^{-1}$ vs. T [92Sob]. τ : dielectric relaxation time.

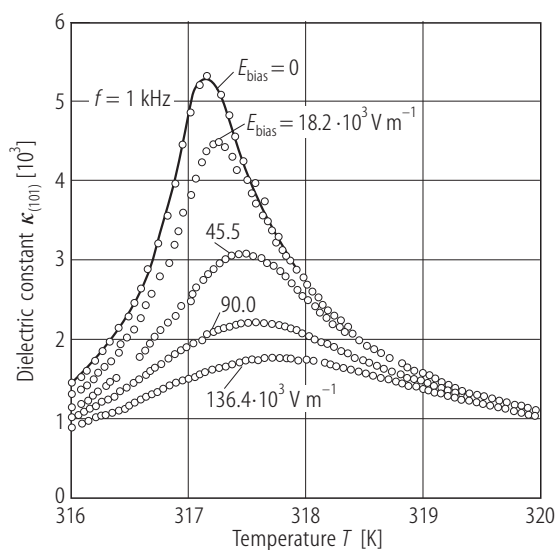


Fig. 38A-1-019. $\text{Te}(\text{OH})_6 \cdot 2\text{NH}_4\text{H}_2\text{PO}_4 \cdot (\text{NH}_4)_2\text{HPO}_4$ (TAAP). $\kappa_{(101)}$ vs. T [90Cac]. Parameter: E_{bias} . $\kappa_{(101)}$: dielectric constant for E perpendicular to (101) face.

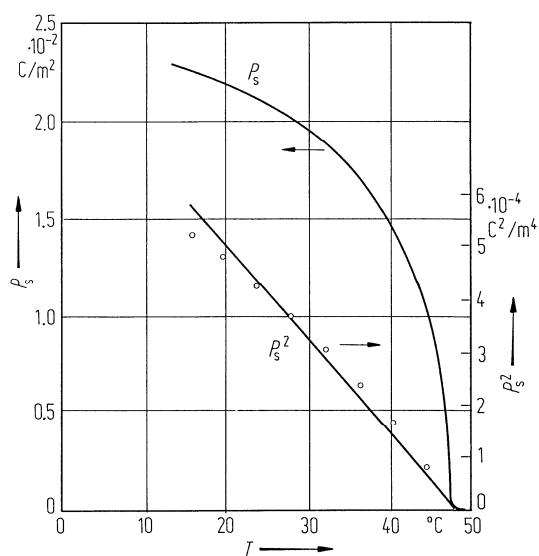


Fig. 38A-1-020. $\text{Te}(\text{OH})_6 \cdot 2\text{NH}_4\text{H}_2\text{PO}_4 \cdot (\text{NH}_4)_2\text{HPO}_4$ (TAAP). P_s , P_s^2 vs. T [84Gui]. P_s : spontaneous polarization measured on (101) plate.

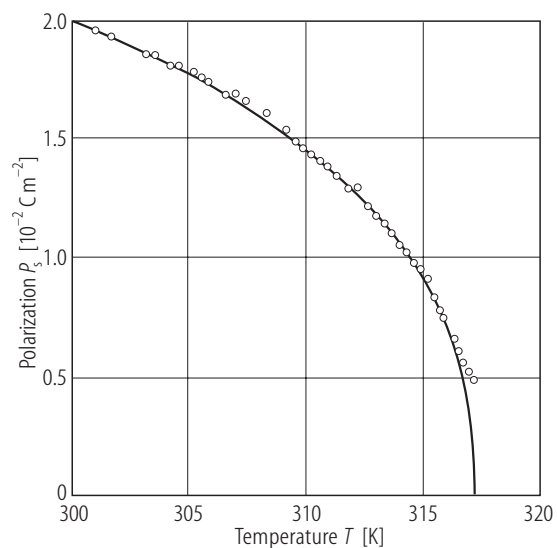


Fig. 38A-1-021. $\text{Te}(\text{OH})_6 \cdot 2\text{NH}_4\text{H}_2\text{PO}_4 \cdot (\text{NH}_4)_2\text{HPO}_4$ (TAAP). P_s vs. T [90Cac].

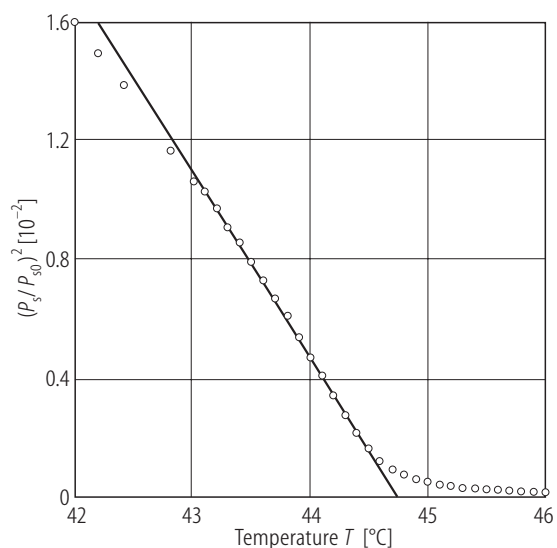


Fig. 38A-1-022. $\text{Te}(\text{OH})_6 \cdot 2\text{NH}_4\text{H}_2\text{PO}_4 \cdot (\text{NH}_4)_2\text{HPO}_4$ (TAAP). $(P_s/P_{s0})^2$ vs. T [96Fer]. P_{s0} : saturated spontaneous polarization: $P_{s0} = 2.12 \cdot 10^{-2} \text{ C m}^{-2}$.

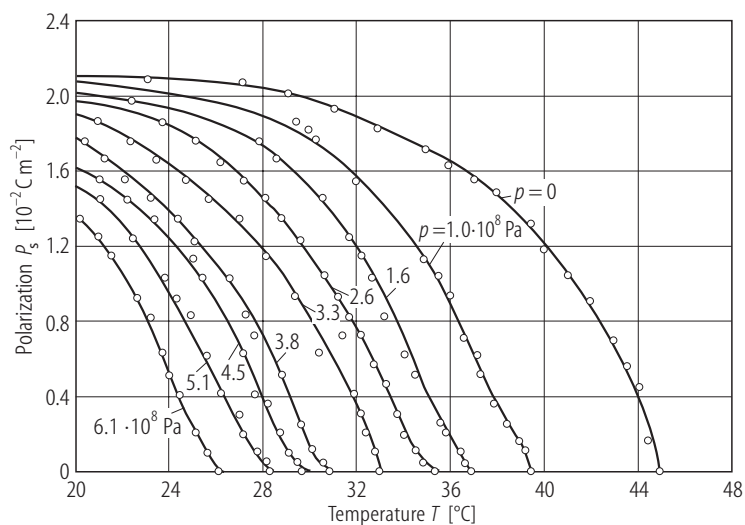


Fig. 38A-1-023. $\text{Te}(\text{OH})_6 \cdot 2\text{NH}_4\text{H}_2\text{PO}_4 \cdot (\text{NH}_4)_2\text{HPO}_4$ (TAAP). P_s vs. T [90Sha2]. Parameter: p .

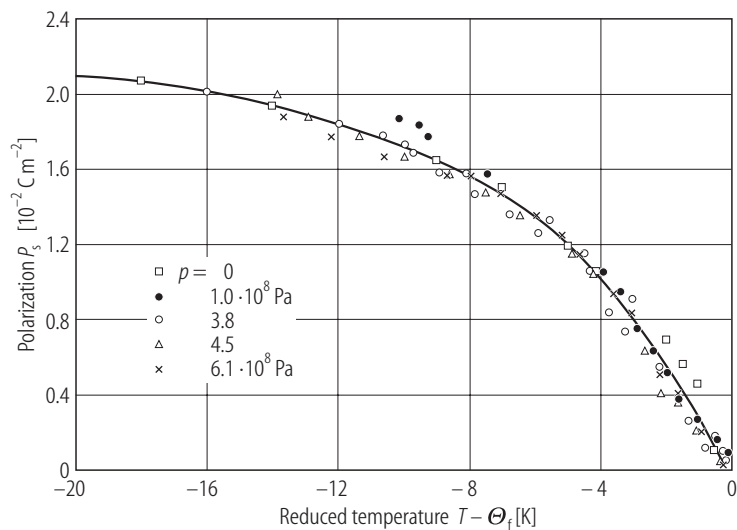


Fig. 38A-1-024. $\text{Te}(\text{OH})_6 \cdot 2\text{NH}_4\text{H}_2\text{PO}_4 \cdot (\text{NH}_4)_2\text{HPO}_4$ (TAAP). P_s vs. $T - \Theta_f$ [90Sha2]. Parameter: p .

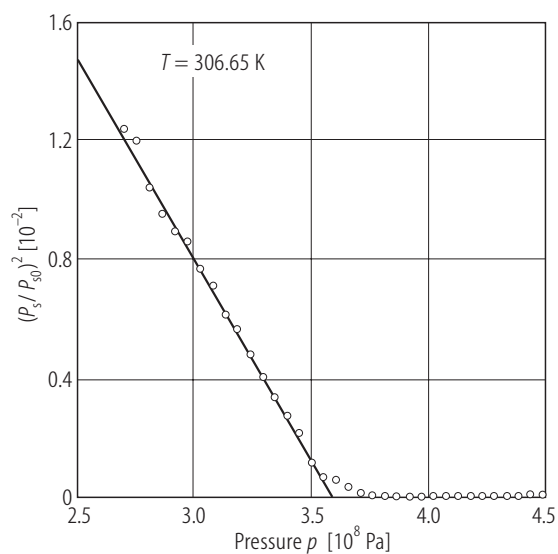


Fig. 38A-1-025. $\text{Te}(\text{OH})_6 \cdot 2\text{NH}_4\text{H}_2\text{PO}_4 \cdot (\text{NH}_4)_2\text{HPO}_4$ (TAAP). $(P_s/P_{s0})^2$ vs. p at 306.65 K [96Fer]. P_{s0} : saturated spontaneous polarization; $P_{s0} = 2.12 \cdot 10^{-2} \text{ C m}^{-2}$.

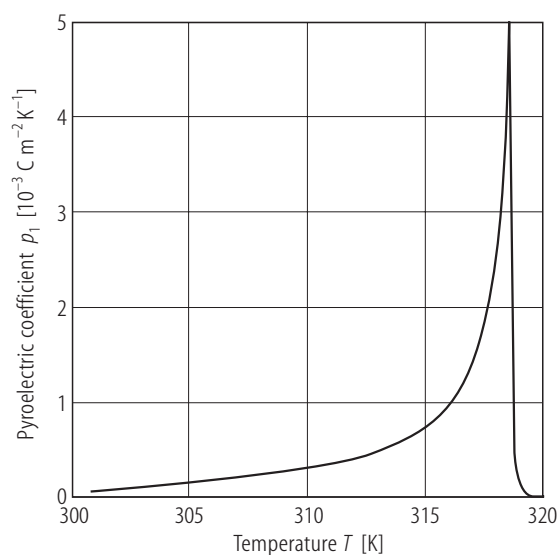


Fig. 38A-1-026. $\text{Te}(\text{OH})_6 \cdot 2\text{NH}_4\text{H}_2\text{PO}_4 \cdot (\text{NH}_4)_2\text{HPO}_4$ (TAAP). p_1 vs. T [91Cza]. p_1 : pyroelectric coefficient measured perpendicular to (101) face.

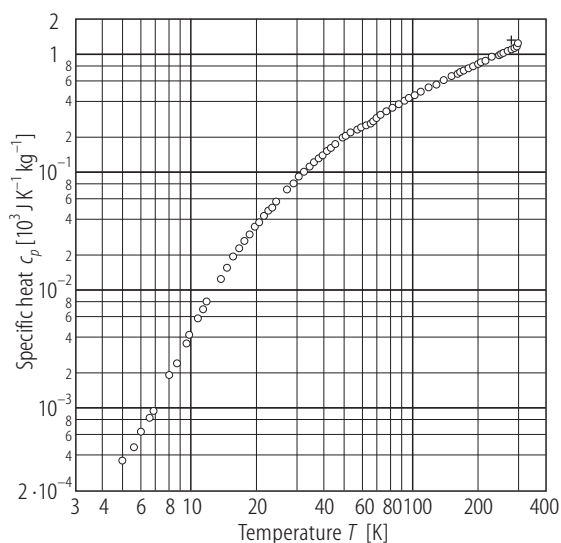


Fig. 38A-1-027. $\text{Te}(\text{OH})_6 \cdot 2\text{NH}_4\text{H}_2\text{PO}_4 \cdot (\text{NH}_4)_2\text{HPO}_4$ (TAAP). c_p vs. T [84Gui]. c_p : specific heat capacity at constant pressure. Circle: adiabatic calorimeter method; plus sign: pyroelectric method.

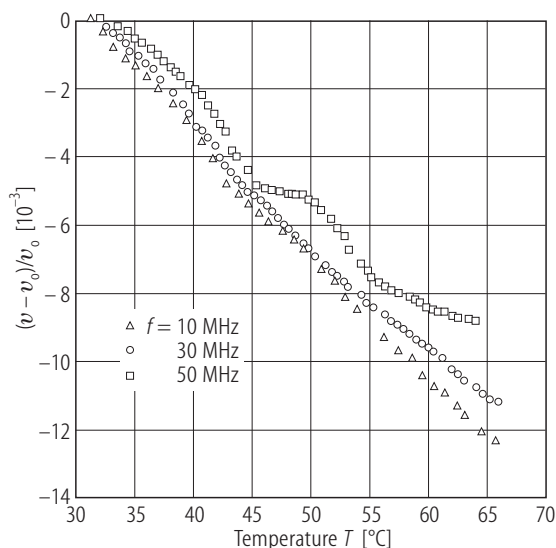


Fig. 38A-1-028. $\text{Te}(\text{OH})_6 \cdot 2\text{NH}_4\text{H}_2\text{PO}_4 \cdot (\text{NH}_4)_2\text{HPO}_4$ (TAAP). $(v - v_0)/v_0$ vs. T [91Ban]. Parameter: f : v : longitudinal ultrasonic wave velocity perpendicular to (101). v_0 : v at 31 °C.

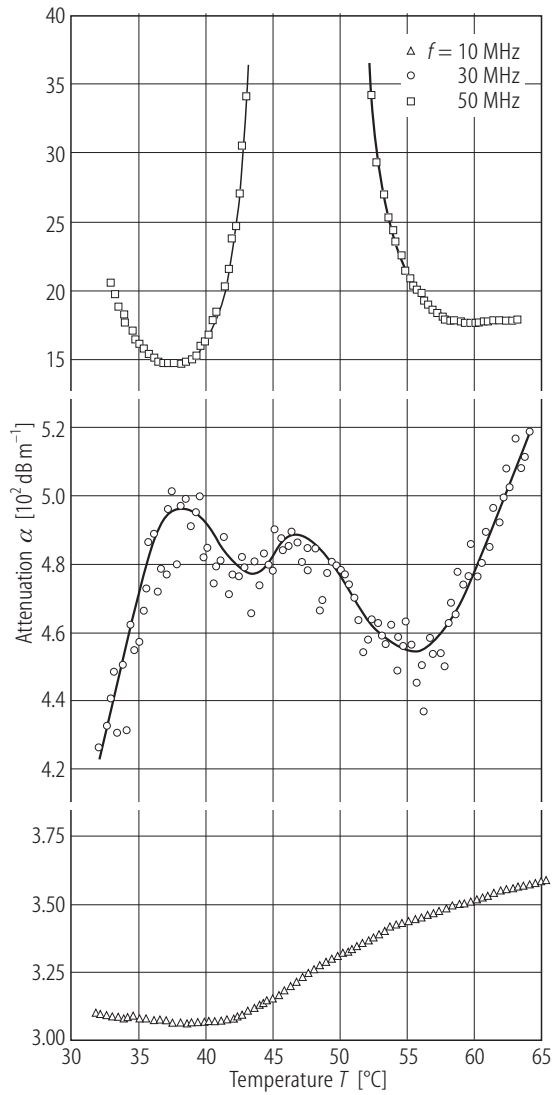


Fig. 38A-1-029. $\text{Te}(\text{OH})_6 \cdot 2\text{NH}_4\text{H}_2\text{PO}_4 \cdot (\text{NH}_4)_2\text{HPO}_4$ (TAAP). α vs. T [91Ban]. Parameter: f . α : attenuation coefficient of longitudinal ultrasonic wave perpendicular to (101) face.

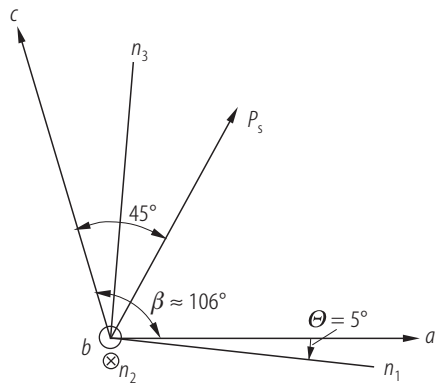


Fig. 38A-1-030. $\text{Te}(\text{OH})_6 \cdot 2\text{NH}_4\text{H}_2\text{PO}_4 \cdot (\text{NH}_4)_2\text{HPO}_4$ (TAAP). Orientation of principal axes of optical indicatrix [94Prz, 84Gui]. Rotation of the optical indicatrix with temperature: see Fig. 38A-1-031.

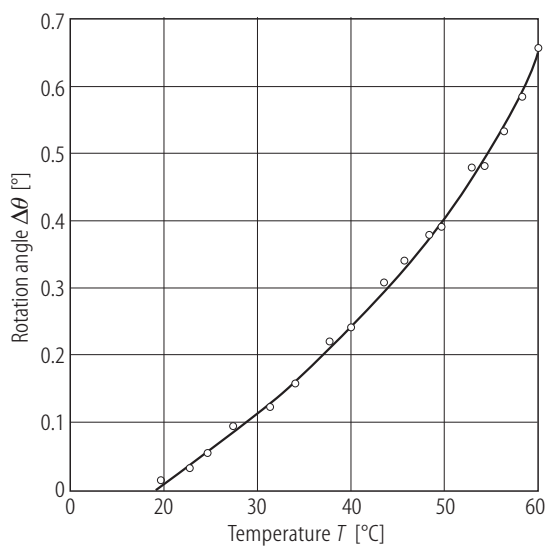


Fig. 38A-1-031. $\text{Te}(\text{OH})_6 \cdot 2\text{NH}_4\text{H}_2\text{PO}_4 \cdot (\text{NH}_4)_2\text{HPO}_4$ (TAAP). $\Delta\theta$ vs. T [84Gui]. $\Delta\theta$: rotation angle of optical indicatrix. See Fig. 38A-1-030.

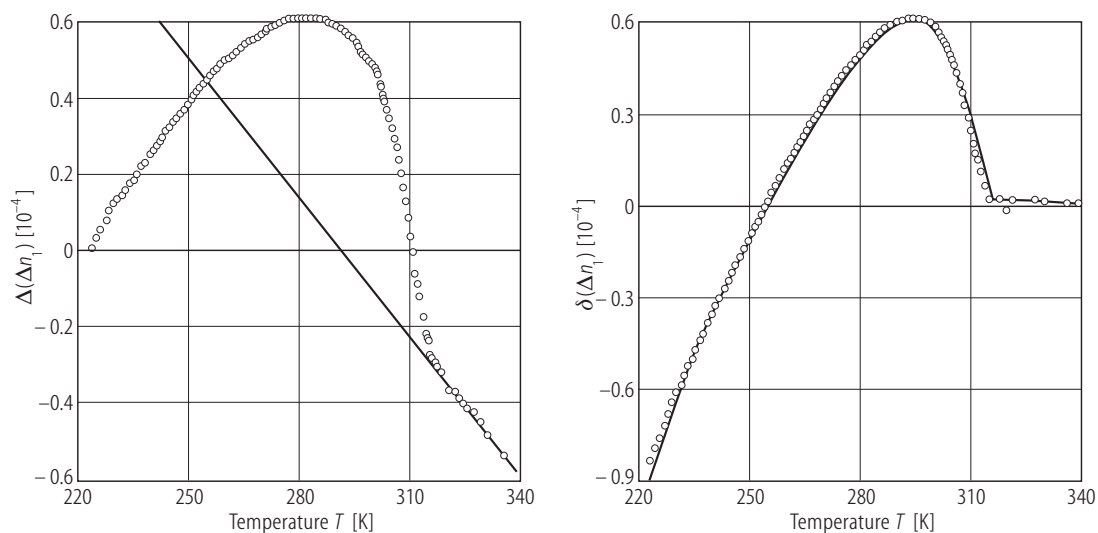


Fig. 38A-1-032. $\text{Te}(\text{OH})_6 \cdot 2\text{NH}_4\text{H}_2\text{PO}_4 \cdot (\text{NH}_4)_2\text{HPO}_4$ (TAAP). $\Delta(\Delta n_1)$, $\delta(\Delta n_1)$ vs. T [94Prz]. $\lambda = 632.8$ nm. $\Delta(\Delta n_1) = \Delta n_1(T) - \Delta n_1(298 \text{ K})$, $\Delta n_1 = |n_2 - n_3|$. $\delta(\Delta n_1)$: deflection of Δn_1 from that of the extrapolated values of phase I. n_1, n_2, n_3 : principal refractive indices. See Fig. 38A-1-030. Full line: extrapolated value from the phase I.

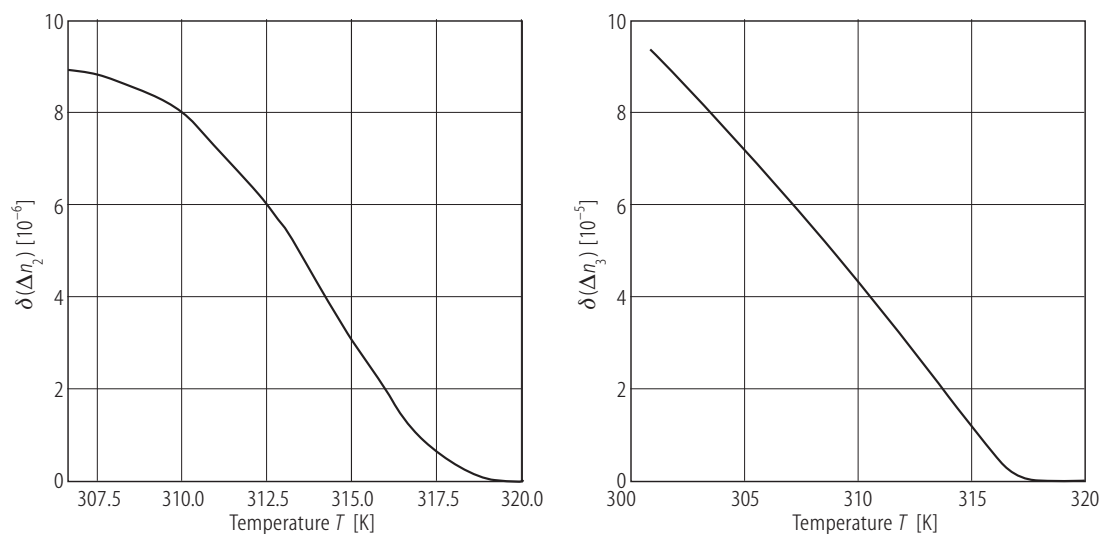


Fig. 38A-1-033. $\text{Te}(\text{OH})_6 \cdot 2\text{NH}_4\text{H}_2\text{PO}_4 \cdot (\text{NH}_4)_2\text{HPO}_4$ (TAAP). $\delta(\Delta n_2)$, $\delta(\Delta n_3)$ vs. T [94Prz]. $\lambda = 632.8$ nm. $\delta(\Delta n_i)$: deflection of Δn_i from that of the extrapolated values of the phase I. $\Delta n_2 = |n_3 - n_1|$, $\Delta n_3 = |n_1 - n_2|$. n_1, n_2, n_3 : principal refractive indices; see Fig. 38A-1-030.

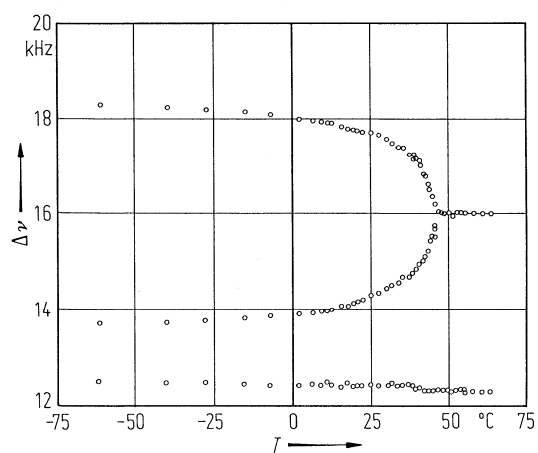


Fig. 38A-1-034. $\text{Te}(\text{OH})_6 \cdot 2\text{NH}_4\text{H}_2\text{PO}_4 \cdot (\text{NH}_4)_2\text{HPO}_4$ (TAAP). $\Delta \nu$ vs. T [84Gai]. $\Delta \nu$: ^{31}P chemical shift. $\nu_L = 81$ MHz.

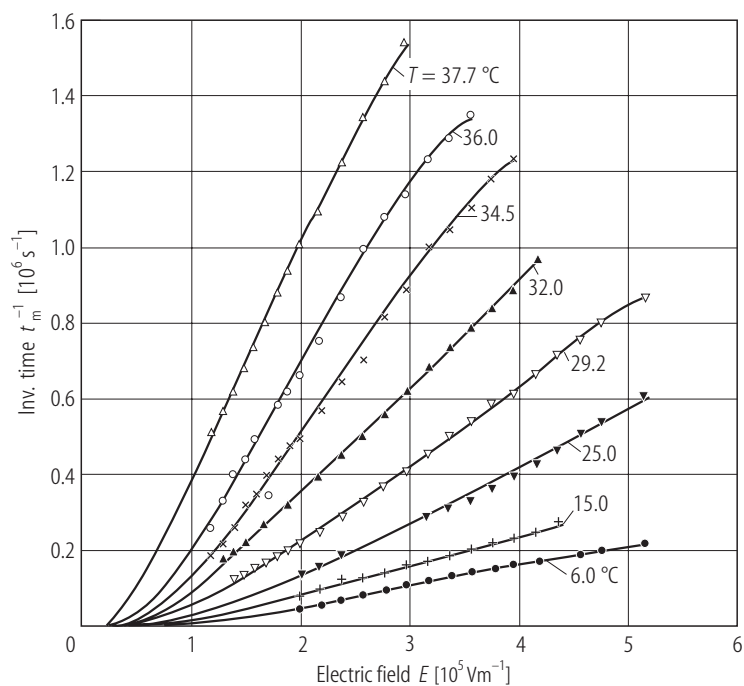


Fig. 38A-1-035. $\text{Te}(\text{OH})_6 \cdot 2\text{NH}_4\text{H}_2\text{PO}_4 \cdot (\text{NH}_4)_2\text{HPO}_4$ (TAAP). t_m^{-1} vs. E [91Sha]. Parameter: T . t_m : time corresponding to the maximum switching current.